

УДК 621.396.96

O. Sukharevsky, V. Vasilets, I. Ryapolov, M. Brechka

Ivan Kozhedub Kharkiv National Air Force University, Kharkiv

SCATTERING CHARACTERISTICS OF Mi-8MT HELICOPTER BASED ON MEASUREMENTS OF OBJECT SCALE MODEL IN AN ANECHOIC CHAMBER

In the paper the scattering characteristics estimation for scale model of Mi-8MT helicopter was carried out for measurements in an anechoic chamber. The description of the experimental measurement system, the methodology of measurement, and the analysis of obtained experimental results are represented. In addition, the features of scattering characteristics are obtained and helicopter design influence are estimated for scattering characteristics of test model. The scattering characteristics of the Mi-8MT were calculated numerically also. The calculations are based on the integral representations of classical electrodynamics and high-frequency asymptotics of scattered fields. These results show an acceptable coincidence between the theory-obtained values and experimental data and confirm the ability of using proposed experimental method of scattering characteristics estimation for aerial object models with complex shape.

Keywords: anechoic chamber, scattering characteristics, backscattering pattern, scale model, radar cross-section.

Introduction

Problem statement. Base characteristics calculation for radar visibility and, particularly, radar cross-section (RCS) is a difficult problem. The variety of aerial designs, layouts, and materials, consideration of helicopter rotors increase essentially the difficulty of obtaining scattering characteristics [1].

Related works analysis. Development of the modern computer technologies allows the direct numerical calculation of Maxwell's equations and obtaining scattering characteristics of aerial objects with complex shape. All re-reflections between different object parts must be taken into consideration. Fig. 1 shows the most common EMW scattering ways in a helicopter.



Fig. 1. Most common EMW scattering ways in a helicopter

Despite the progress in electrodynamic calculation methods for object scattering characteristics [2–9] whose capabilities increase along with the computing technologies, the currently existing calculation methods are not yet to replace physical measurements completely, especially if the object has complex shape as a

helicopter. Taking physical measurements is crucial, especially for verification and improvement of calculation methods.

Presently, among the known methods [2; 4; 10; 11], the following are most commonly used at this time:

- RCS ground tests of real objects (specifically, measurement systems of 2nd Research Institute of Ministry of Defense, Russia; MVG Microwave Vision Group [12], Howland Company [13], USA);
- scale model RCS measurement in an anechoic chamber [14; 15].

Thus, the problem of accurate obtaining of scattering characteristics can't be solved by theoretical methods only.

There are two most common RCS testing area methods:

- static (a special ground tests, where the target is installed on an elevated rotation tool);
- flying around the radar that it tracks the target, while simultaneously measuring its scattering characteristics.

In the flying around radar all tests are carried out in the real-life conditions with all essential radar factors: actual radar power, the sounding signal type, the signal processing method, the presence of ghost reflections, actual jamming environment.

However, there are factors that prevent common usage of this method: difficulty of the maneuver required for the proper target probing, inaccuracies in determining the probing direction, long distances, high cost, poor result precision.

All static types of radar testing area can be sort into two categories:

- areas where the ground surface is not a forming factor in the scattered field, i.e. free space areas;
- areas that use the ground surface as a reflected surface.

The first case involves taking all measures to eliminate the ground reflection, which is achieved by elevating both the radar antenna and the target to the maximum height possible, and installation of the special screens.

In the second case, on the contrary, the antenna is placed near ground and the target is elevated to the height of the first interference maximum. This approach allows reducing the testing area size substantially, but usage of such testing areas causes difficulties measuring horizontal and circular signal polarization, thus such measures are carried out in the free space testing areas [16].

Anechoic chambers are widely used in scattering characteristics obtaining for aerial objects. An anechoic chamber is a room with interior surfaces covered with radar absorbing material (RAM) to minimize surface reflections and create within certain space of the chamber – the an-echoic zone – with a specified low level of reflections, i.e. conditions close to free space testing area. An anechoic chamber also allows to make almost all types of radio-measurements, specifically obtaining antenna parameters, radar target scattering characteristics, aircraft radio facilities testing, etc. In many cases, using an anechoic chamber allows to minimize or omit field testing completely and save time and funds substantially. Radar testing an anechoic chamber is completely free from various natural or artificial jamming, that allows to make precise measurement.

The paper objective is to determine the features of scattering characteristics for a scale model of Mi-8MT helicopter evaluate the impact of the layout and design to the test model scattering characteristics, based on anechoic chamber physical experiment data.

An anechoic chamber description

Physical experiment was carried out in the anechoic chamber at Karazin Kharkiv National University.

Characteristics of the chamber are follows:

- dimensions of the anechoic chamber with curved walls $8,3 \times 5,2 \times 4 \text{ m}^3$;
- measurement accuracy class – 1, which means the chamber was designed for precise radio system measurements;
- inner surfaces are covered with tight-fit 8400 pyramids made of RAM; each pyramid have height about 320 mm, nose angle is $\alpha=30^\circ$. Pyramids of that size with incident angles $\theta=0\dots40^\circ$ give the number of reflections no less than 4, and each reflection gives absorbing of 5...12 dB. RAM is radar absorbent foam glass with electromagnetic attenuation 2–3 dB/cm for signal frequency 2375 MHz. Its inorganic composition, low density, closed cellular structure of the carbonaceous foam glass ensure

the stability of its physical features, efficacy and durability in a wide temperature and humidity range. High quality of the carbonaceous foam glass is defined of its closed cellular structure that prevents rules out the moisture absorption and ensures stable physical properties at low temperature or high humidity.

Experimental measuring system description

Fig. 2 shows the layout of the experimental test to estimate the scattering characteristics of radar targets in the anechoic chamber. Fig. 3 shows the anechoic chamber equipment photos. Fig. 4 shows the photo of measuring system.

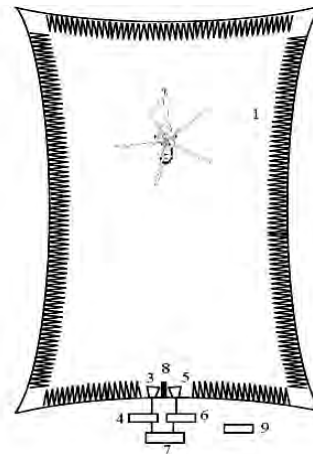


Fig. 2. Layout of the experimental test to estimate the scattering characteristics of radar targets in the anechoic chamber

- (1 – chamber walls covered by pyramid-shaped RAM; 2 – experimental target on the rotation device; 3 – transmitting antenna P6-23A; 4 – microwave oscillator G4-111; 5 – receiving antenna P6-23A; 6 – voltage ratio meter V8-7; 7 – pulse oscillator G5-63; 8 – screen; 9 – oscilloscope)

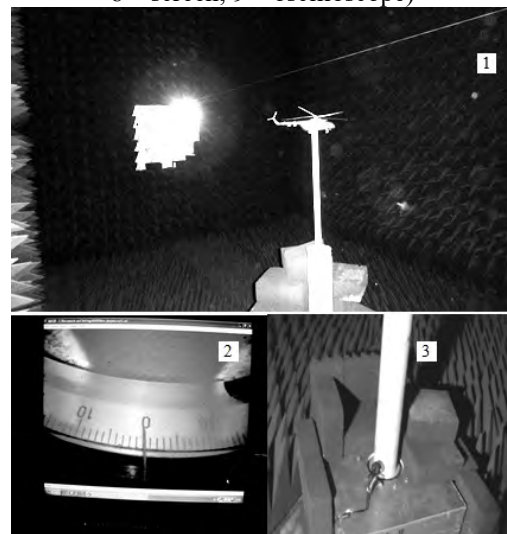


Fig. 3. Anechoic chamber equipment: 1 – experimental target on dielectric column of the rotation device; 2, 3 – rotation device indicating the model's angular position

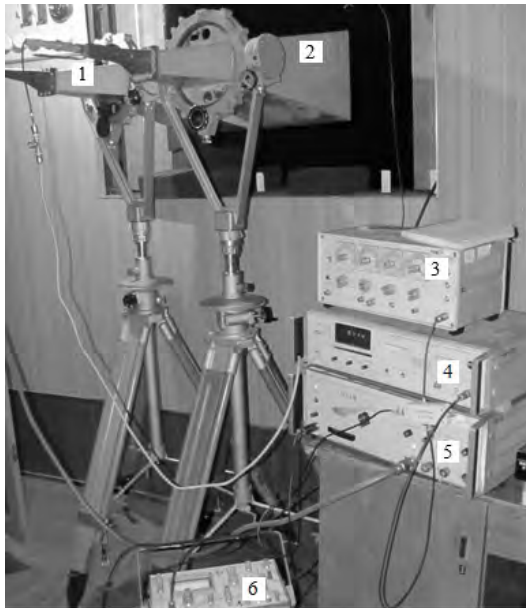


Fig. 4. Measuring system:

- 1 – transmitting antenna P6-23A; 2 – receiving antenna P6-23A; 3 – pulse oscillator G5-63; 4 – voltage ratio meter V8-7; 5 – microwave oscillator G4-111; 6 – oscilloscope

Experimental target is mounted inside the chamber, on the rotation device that is a single frame containing the dielectric column rotation gear, rotary tool drive for the rotation gear, angular position indicator.

Rotation device is covered by the same RAM type as the chamber walls.

Microwave oscillator G4-111 is a source of ultra-high frequency waves with of non-calibrated output power.

Pulse oscillator G5-63 is a source of simple types of output pulse pattern and is intended for external modulation of microwave oscillations.

Voltage ratio meter V8-7 is a measuring device for ratio of voltage in alternate current, also an amplifier for low voltage in alternate current, and as voltage converter with the ability for linear phase-sensitive conversion of these voltages into a direct current voltage, with output signal digital indication in some relative units. Analogue outputs for alternate and direct currents allow to use this device in automatic monitoring system with the data recording.

Measuring antenna P6-23A works at the frequency range of 1,0...12,0 GHz and serves for:

- power flow density measuring;
- RCS and antenna gain measuring;
- generating an electromagnetic field with specified power density, and other antenna measurements.

The radiation pattern sidelobe is no more than 10 dB in the operating frequency range. The tripod and orientation mechanism enable azimuthal rotation of the antenna in 360° range, antenna elevation angle from +

90° to -30°, rotation angle of polarization plane in range from 0° to 190°, smooth vertical change.

Equipment and antenna calibration was carried out using the reference metal spheres (fig. 5) whose radii and RCSs are known since a sphere's RCS doesn't depend on radar beam relative position, and is equal to its cross-section square in high frequency range.



Fig. 5. Reference spheres

The model aircraft's RCS is the oscillating function of the probing signal's frequency in frequency range used for tests. This is determined by dependence of phase difference signals scattered by different parts of the model's surface from signal frequency, changing Fresnel zones on the model's surface sensitive to the probing signal's frequency changes [17; 18], and general compliance of the equipment used in the modeling experiment. Moreover, RCS determination technique does not consider such factors as, for example, transmitting and receiving antennas abilities to transmit and receive a wave with specific polarization only. In the bistatic receiving used in the anechoic chamber model experiment, transmitting and receiving antennae's polarization does not coincide, thus only a part of the scattered signal would be received, and the obtained RCS would be less than the theoretical value, and this fact must be taken into consideration [3]. Microwave oscillator power in aggregate with the rest of the equipment specs compliance, which is determined experimentally, is important for measurement of low- visible model RCS. Therefore, the choice of the probing signal frequency must be determined experimentally in the microwave oscillator's maximum energy zone to find the maximum input signal power. This allows to satisfy the requirements to the microwave oscillator power in low-visible target tests, and to decrease errors caused by lack of equipment compliance [19].

Scattering pattern measurement method for Mi-8MT helicopter model in an anechoic chamber

Mi-8MT helicopter model used in tests is a plastic 1:72 scaled model of the real helicopter. Once the

model has been assembled (with the exception of the glass cockpit enclosure), a 15 micron layer of aluminum was applied by means of vacuum plating, which allowed to use the model in anechoic chamber experiment.

A laser level gage (fig. 6, 7) was used to point the antenna directly to the reference sphere center and to the target during the experiment itself. The elevation angle in tests was -3 degrees, azimuth change step was 1 degree, azimuth was counted from the object nose (0 degrees is probing to the nose, 180 degrees is probing the tail), wavelength is 3.35 cm.



Fig. 6. Laser mark on the target

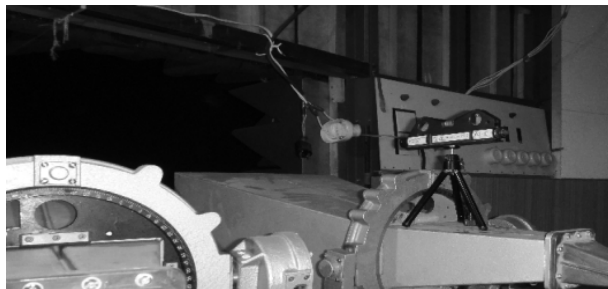


Fig. 7. Laser level gage

The anechoic chamber-based experiment to measure the radar object scattering pattern was carried out by following way. The measuring system equipment was turned on and warmed up during 30 minutes to keeping equipment stability. Next step was noise level estimation and scale calibration. The tested object was placed in the anechoic chamber at the same distance as reference scatterers (spheres). The dielectric column with the installed target was joined mechanically with the rotation device that allowed to change the azimuthal angle. The experimental results were tabulated, averaged out, and RCS value was determined.

After each measurement section the equipment was re-calibrated and results compared with received earlier, to ensure correct and stable equipment parameters.

The analysis of experimental results

To validate the performance capabilities of proposed method [20–24] for calculation of aerial object RCS, scattered patterns obtained in calculations and

experiment were compared for Mi-8MT multi-purpose helicopter.

Experimental measurements for the model Mi-8MT were taken at the anechoic chamber described above.

Fig. 8 shows Mi-8MT RCS experimental data averaged over azimuth 0°...360° compared with the calculated scattering characteristics [20–24].

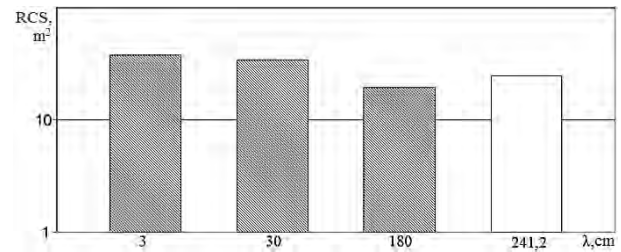


Fig. 8. Mi-8MT helicopter averaged RCS versus probing signal wavelength (λ) (dashed columns are calculated data, white column is experimental data)

The experimental value (at wavelength 241,2 cm) is closer to the RCS estimate for wavelength 180 cm. This fact tells about adequacy of the numerical calculations. Probing signal wavelength influence on the averaged RCS of Mi8-MT helicopter is not crucial. Thus, the good coincide of calculation and experimental data (fig. 8) validates additionally the proposed experimental method for RCS estimation of aerial objects with complex shape.

Fig. 9 shows experimental and calculated RCS of Mi8-MT helicopter versus azimuth aspect angle.

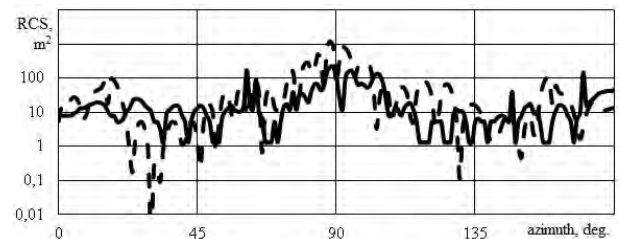


Fig. 9. RCS of Mi-8MT helicopter versus azimuth aspect angle (solid line – experiment, cross-hatching line – calculation)

The experimental model included the cockpit and side windows. Experimental RCS value σ was scaled up to the RCS of a real object using the equation:

$$\sigma = \sigma'p^2,$$

where p is the scale factor ($p=72$).

The graphs in fig.9 show that for nose azimuths there are multiple reflections between control panels and the cockpit partition instead of a direct mirror reflection. Experimental RCS values have good coincide with the numerical calculation data (fig. 9). Some differences can be seen for the nose azimuths since the model cockpit windows were assumed as an ideal reflected surface.

Analyzing the obtaining experimental data it can be concluded that experimental model RCS value for side sounding (azimuth near 90°) is lower than for calculation model due to errors in equipment calibration for corresponding angles.

Conclusion

The paper presents the experimental method for estimation of scattering patterns of a 1:72 scaled Mi-8MT helicopter model. The model was made of plastic and vacuum-covered with 15 micron aluminium, that allowed to use this model in the anechoic chamber experiment. Measurements were taken for wavelength 3,35 cm. Average RCS values are: for the nose aspect angles – 11 m², for the side aspect angles – 35 m², for the tail aspect angles – 16 m². Considering similarity principle, these values match to the RCS of an real helicopter for sounding wavelength at 241,2 cm. Obtained numerical calculations show small differences for the averaged circle RCS values in SHF and UHF bands.

Numerical calculation results and experimental data have good coincide. Differences between numerical and experimental data can be explained by using perfectly conducting surface for cockpit windows in calculation model and some inequality in elevation angles for numerical calculations and the experiment. Difference occurs at the nose aspect angles due to multiple reflections between control panels and the cockpit partition in experiment and a direct mirror reflection in numerical calculation. Experimental RCS value σ' was scaled up to that of real object with scale factor $p=72$. Experimental scattering pattern is qualitatively similar and consistent with the calculated scattering pattern.

Analysis of the represented dependencies allows to conclude that experimental and calculation data match is satisfactory. Lower experimental RCS values were induced by bistatic reception (with bistatic angle 2,1°).

Good coinciding of calculated and experimental data (less than 11%) validates additionally the proposed experimental method for RCS estimation of aerial objects with complex shape.

References

1. Анишко О.Б. *Аэродинамический облик, радиолокационная и инфракрасная заметность самолетов военного назначения при их обнаружении: монография* / О.Б. Анишко, В.Г. Башинский, Е.А. Украинец; под ред. О.Б. Анишко. – Запорожье: изд. АО "Мотор Сич", 2013. – 250 с.
2. Knott E.F. *Radar Cross Section, 2nd Edition* / E.F. Knott, J.F. Shaeffer, M.T. Tuley. – Raleigh, NC: SciTech Publishing, Inc, 2004. – 653 p.
3. *Computer Simulation of Aerial Target Radar Scattering Recognition, Detection and Tracking* / Shirman Ya.D. et al.; Ya.D. Shirman (ed). – Norwood, M.A.: Ar-tech House, 2002. – 382 p.
4. Львова Л.А. *Радиолокационная заметность летательных аппаратов* / Л.А. Львова. – Снежинск: Изд-во РФЯЦ – ВНИИТФ, 2003. – 232 с.
5. Уфимцев П.Я. *Теория дифракционных краевых волн в электродинамике* / П.Я. Уфимцев. – М.: Бином, 2007. – 366 с.
6. Gibson W.C. *The Method of Moments in Electromagnetics* / W.C. Gibson. – Boca Raton London New York: Chapman & Hall / Taylor & Francis Group, 2008. – 288 p.
7. *Рассеяние электромагнитных волн воздушными и наземными радиолокационными объектами: монография* / О.И. Сухаревский, В.А. Василец, С.В. Кукобко и др.; под ред. О.И. Сухаревского. – Х.: ХУ ВС, 2009. – 468 с.
8. *Ultrawideband Radar. Application and Design* / J.D. Taylor, O.I. Sukharevsky, V.A. Vasilets and others // Edited by James D. Taylor. – Boca Raton, London, New York: SRC Press Taylor & Francis Groupe, 2012. – 520 p.
9. Залевский Г.С. *Радиолокационные дальностные портреты крылатых ракет в различных диапазонах длин волн* / Г.С. Залевский, В.А. Василец, О.И. Сухаревский // *Прикладная радиоэлектроника*. – 2014. – Т. 13, № 1. – С. 20-28.
10. Майзельс Е.Н. *Измерение характеристик рассеяния радиолокационных целей* / Е.Н. Майзельс, В.А. Торгованов; под ред. М.А. Колосова. – М.: Сов. радио, 1972. – 232 с.
11. *Радиоэлектронные системы: Основы построения и теория. Справочник. Изд. 2-е, перераб. и доп.* / Под ред. Я.Д. Ширмана. – М.: Радиотехника, 2007. – 512 с.
12. *MVG Microwave Vision Group. Solutions for Aerospace and Defense. [Электронный ресурс]. – Режим доступа до ресурсу: <http://www.microwavevision.com/panels/industries/aerospace-defense>.*
13. *The Howland Company. Radar Cross-Section (RCS) Range Design & Evaluation. – [Электронный ресурс]. – Режим доступа до ресурсу: http://www.thehowlandcompany.com/radar_stealth/RCS-ranges.htm.*
14. *Damaskos, Inc. Material Measurement Solution. Anechoic Chamber. [Электронный ресурс]. – Режим доступа до ресурсу: <http://www.damaskosinc.com/products.htm>.*
15. *Безэховая камера СВЧ сантиметрового диапазона и методика определения ее основных характеристик* / Э.Ф. Каменский, И.Г. Леонов, Д.В. Максютя и др. // *Сборник научных трудов Харьковского военного университета*. – Х., 2000. – № 4(30). – С. 72-78.
16. Ваганов Р.Б. *Основы теории дифракции* / Р.Б. Ваганов, Б.З. Каценелембаум. – М.: Наука, 1982. – 272 с.
17. Mentzer J.R. *Scattering and Diffraction of Radio Waves* / J.R. Mentzer. – London & New York: Pergamon Press, 1955. – 340 p.
18. *Эффективная поверхность рассеяния (ЭПП) объектов с неидеально отражающей поверхностью, имеющей изломы* / О.И. Сухаревский, В.А. Василец, С.А. Горельишев и др. // *Зарубежная радиоэлектроника*. – М., 2001. – № 6. – С. 41-48.
19. Youssef N.N. *Radar Cross Section of Complex Targets* / N.N. Youssef // *IEEE Tr. on AP*. – 1989. – Vol. 77, No 5. – P. 722-734.

20. Розробка методики оцінки радіолокаційних характеристик вертолітної техніки Повітряних Сил Збройних Сил України / Я.О. Белевицук, М.М. Бречка, В.О. Василець і др. // Наука і техніка Повітряних Сил Збройних Сил України. – 2011. – № 1. – С. 83-87.

21. Розрахунок радіолокаційних характеристик моделі багатоцільового вертольоту Мі-8МТ / Я.О. Белевицук, М.М. Бречка, В.О. Василець і др. // Системи озброєння і військова техніка. – 2011. – № 2. – С. 18-22.

22. Ряполов І.Є. Високочастотний асимптотичний метод розрахунку вторинного випромінювання моделі безпілотного літального апарату / І.Є. Ряполов // Наука і техніка Повітряних Сил Збройних Сил України. – 2016. – № 3(24). – С. 86-89.

23. Ряполов І.Є. Високочастотний метод расчета рассеяния вторичного излучения диэлектрических частей модели беспилотного летательного аппарата / И.Е. Ря-

полов, В.А. Василец, О.И. Сухаревский // Системи обробки інформації. – Х.: ХУПС, 2014. – Вип. 2(118). – С. 58-62.

24. Сухаревський О.І. Оцінювання параметрів зон виявлення безпілотного літального апарату "Орлан-10" радіолокаційними засобами самохідного зенітного ракетного комплексу 9К33МЗ "Оса-АКМ" / О.І. Сухаревський, В.О. Василець, І.Є. Ряполов // Наука і техніка Повітряних Сил Збройних Сил України. – 2016. – № 4(25). – С. 33-38.

Надійшла до редколегії 12.01.2017

Рецензент: д-р техн. наук, ст. наук. співробітник Г.С. Залевский, Харківський національний університет Повітряних Сил ім. І. Кождуба, Харків.

ОЦІНКА ХАРАКТЕРИСТИК ВТОРИННОГО ВИПРОМІНЮВАННЯ МАСШТАБНОЇ МОДЕЛІ БАГАТОЦІЛЬОВОГО ВЕРТОЛЬОТА МІ-8МТ, ОТРИМАНОЇ ПРИ ПРОВЕДЕННІ ВИМІРЮВАНЬ У БЕЗЛУННІЙ КАМЕРІ

О.І. Сухаревський, В.О. Василець, І.Є. Ряполов, М.М. Бречка

У статті проведена оцінка характеристик вторинного випромінювання масштабної моделі багатоцільового вертольоту Мі-8МТ, що отримана при проведенні вимірювань в безлунній камері. Представлений опис експериментального вимірювального комплексу, методика проведення вимірювань і проведений аналіз результатів експериментальних досліджень. Крім цього, виявлені особливості вторинного випромінювання і оцінений вплив компоувальної схеми вертольоту на характеристики розсіювання досліджуваної моделі. Отримані характеристики розсіювання вертольоту Мі-8МТ шляхом математичного моделювання із застосуванням методу, який заснований на інтегральних уявленнях класичної електродинаміки і короткохвильових асимптоти, що входять до них полів. Представлені результати показують задовільний збіг теоретичних значень і експериментальних даних і підтверджують можливість використання розробленої експериментальної методики для визначення вторинного випромінювання моделей складних аеродинамічних об'єктів.

Ключові слова: безлунна камера, вторинне випромінювання, діаграма зворотного вторинного випромінювання, масштабна модель, ефективна поверхня розсіювання.

ОЦЕНКА ХАРАКТЕРИСТИК ВТОРИЧНОГО ИЗЛУЧЕНИЯ МАСШТАБНОЙ МОДЕЛИ МНОГОЦЕЛЕВОГО ВЕРТОЛЕТА МИ-8МТ, ПОЛУЧЕННОЙ ПРИ ПРОВЕДЕНИИ ИЗМЕРЕНИЙ В БЕЗЭХОВОЙ КАМЕРЕ

О.И. Сухаревский, В.А. Василец, И.Е. Ряполов, М.М. Бречка

В статье проведена оценка характеристик вторичного излучения масштабной модели многоцелевого вертолета Ми-8МТ, полученной при проведении измерений в безэховой камере. Представлено описание экспериментального измерительного комплекса, методика проведения измерений и проведен анализ результатов экспериментальных исследований. Кроме этого, выявлены особенности вторичного излучения и оценено влияние компоновочной схемы вертолета на характеристики рассеяния исследуемой модели. Получены характеристики рассеяния вертолета Ми-8МТ путем математического моделирования с применением метода, основанного на интегральных представлениях классической электродинамики и коротковолновых асимптот входящих в них полей. Представленные результаты показывают удовлетворительное совпадение теоретических значений и экспериментальных данных и подтверждают возможность использования разработанной экспериментальной методики для определения вторичного излучения моделей сложных аэродинамических объектов.

Ключевые слова: безэховая камера, вторичное излучение, диаграмма обратного вторичного излучения, масштабная модель, эффективная поверхность рассеяния.